Three-Dimensional Solution Structure of the B Domain of Staphylococcal Protein A: Comparisons of the Solution and Crystal Structures†

Hiroaki Gouda,‡ Hidetaka Torigoe,‡,§ Akiko Saito,‖ Moriyuki Sato,‖ Yoji Arata,*,‡ and Ichio Shimada*,‡

Faculty of Pharmaceutical Sciences, University of Tokyo, Hongo, Tokyo 113, Japan, and Tokyo Research Laboratories, Kyowa Hakko Kogyo Co., Ltd., Asahimachi 3-6-6, Machida, Tokyo 194, Japan

Received May 28, 1992; Revised Manuscript Received July 10, 1992

ABSTRACT: The three-dimensional solution structure of the recombinant B domain (FB) of staphylococcal protein A, which specifically binds to the Fc portion of immunoglobulin G, was determined by NMR spectroscopy and hybrid distance geometry–dynamical simulated annealing calculations. On the basis of 692 experimental constraints including 587 distance constraints obtained from the nuclear Overhauser effect (NOE), 57 torsion angle (ϕ, χ^1) constraints, and 48 constraints associated with 24 hydrogen bonds, a total of 10 converged structures of FB were obtained. The atomic root mean square difference among the 10 converged structures is 0.52 ± 0.10 Å for the backbone atoms and 0.98 ± 0.08 Å for all heavy atoms (excluding the N-terminal segment from Thr1 to Glu9 and the C-terminal segment from Gln56 to Ala60, which are partially disordered). FB is composed of a bundle of three α-helices, i.e., helix I (Gln10–His19), helix II (Glu25–Asp37), and helix III (Ser42–Ala55). Helix II and helix III are antiparallel to each other, whereas the long axis of helix I is tilted at an angle of about 30° with respect to those of helix II and helix III. Most of the hydrophobic residues of FB are buried in the interior of the bundle of the three helices. It is suggested that the buried hydrophobic residues form a hydrophobic core, contributing to the stability of FB. On the basis of the results of amide proton exchange experiments performed by observing heteronuclear ^1H–^{15}N NMR spectra, we have concluded that the structure of the bundle of the three helices is retained in the Fc–FB complex in solution. This result is in marked contrast to that of an X-ray crystallographic study of the Fc–FB complex [Deisenhofer, J. (1981) *Biochemistry 20*, 2361–2370], which shows that the Ser42–Glu48 segment is extended and no structural information is available on the Ala49–Lys59 segment. We suggest that crystal contact in the Fc-bound FB is responsible for the disordered structure of the Ser42–Ala55 segment in the crystal.

Protein A, which is a cell wall component of *Staphylococcus aureus*, binds specifically to the Fc portion of immunogobulin G (IgG)[1] from various mammalian species (Langone, 1982). The extracellular part of protein A contains a tandem of 5 highly homologous Fc-binding domains designated as E, D, A, B, and C, each of which comprises about 60 amino acid residues. The C-terminal part is a cell wall binding domain designated as X, which does not bind to the Fc portion and comprises approximately 180 amino acid residues (Sjodahl, 1977a,b; Moks et al., 1986).

The three-dimensional structure of the B domain of protein A (FB) bound to the Fc fragment of human polyclonal IgG has been determined by X-ray crystallographic analysis at 2.8-Å resolution (Deisenhofer, 1981). The electron density for the Fc-bound FB was observed for the Phe6–Glu48 segment; no structural information was available for the segments Ala2–Lys5 and Ala49–Lys59. The crystal data have indicated that two antiparallel helical regions, Gln10–Leu18 and Glu26–Asp37, exist in the Fc-bound FB. It has also been indicated that in the crystal FB forms two contacts with the Fc fragment. It has been suggested that one of the two contacts is a crystal contact.

In a previous study, we have determined on the basis of NMR data the secondary structure of the 60-residue recombinant FB in solution (Torigoe et al., 1990). In marked contrast to the crystal data, the free FB in solution contains three helical regions, Glu9–His19, Glu25–Asp37, and Ser42–Ala55. It has been suggested that a significant conformational change is induced in the C-terminal region of FB when it is bound to the Fc portion of IgG in the crystal (Torigoe et al., 1990).

In the present paper, we report the three-dimensional solution structure of the free FB as determined by NMR and hybrid distance geometry–dynamical simulated annealing calculations. We will also discuss the structure of the Fc-bound FB in solution on the basis of the result of amide proton exchange experiments. The NMR results obtained will be compared with the crystal data, and a possible reason for the differences between the solution and crystal structures will be discussed.

MATERIALS AND METHODS

Sample Preparation. A synthetic gene for FB has been expressed in *Escherichia coli* (Saito et al., 1989). For

† This research was supported in part by special coordination funds for promoting science and technology from the Science and Technology Agency and by grants from the Ministry of Education, Science, and Culture of Japan (62870089 and 63430022).

‡ University of Tokyo.

§ Present address: Laboratory of Gene Bank, Tsukuba Life Science Center, The Institute of Physical and Chemical Research (RIKEN), Tsukuba, Ibaragi 305, Japan.

‖ Kyowa Hakko Kogyo Co., Ltd.

[1] Abbreviations: DSS, sodium 2,2-dimethyl-2-silapentane-5-sulfonate; FB, B domain of staphylococcal protein A; Fc, fragment composed of the C-terminal halves of the heavy chains of immunoglobulin G; HPLC, high-performance liquid chromatography; HOHAHA, homonuclear Hartmann–Hahn spectroscopy; HSQC, heteronuclear single-quantum correlation; HMQC, heteronuclear multiple-quantum correlation; IgG, immunoglobulin G; NMR, nuclear magnetic resonance; NOE, nuclear Overhauser effect; NOESY, two-dimensional NOE correlated spectroscopy; PE-COSY, primitive exclusive COSY; RMS, root mean square; RMSD, RMS difference.

0006-2960/92/0431-9665$03.00/0

nonlabeled FB, *E. coli* strain W3110 containing the expression plasmid for FB was grown in L medium. In order to obtain FB labeled unformly with ^{15}N, *E. coli* W3110 was grown in M9 minimal medium containing $^{15}NH_4Cl$ as the sole nitrogen source. The uniformly labeled FB will hereafter be designated as [^{15}N]FB. The FB proteins were isolated and purified as described previously (Torigoe et al., 1990).

The Fc fragment of human myeloma protein IgG1(κ) Ike-N was prepared by papain digestion at pH 7.0, 37 °C, in 75 mM sodium phosphate buffer which contains 75 mM NaCl, 2 mM EDTA, and 5 mM NaN_3. The protein concentration was 10 mg/mL, and the enzyme concentration was 1.0 mg/mL. The enzyme:substrate ratio (w/w) was 25:1. The incubation time was 6 h. The digestion product of IgG(κ) Ike-N was loaded onto an Affigel protein A column (Bio-Rad) equilibrated with 0.1 M sodium phosphate buffer, pH 8.0, and eluted using 0.1 M citrate buffer, pH 3.0. The final purification of the Fc fragment was performed on a Pharmacia Superose 12 HPLC column equilibrated with 10 mM sodium phosphate buffer, pH 7.2. The purity of the protein preparation was checked by SDS–polyacrylamide gel electrophoresis.

NMR Measurements. NOESY (Jeener et al., 1979) and PE-COSY (Mueller, 1987) spectra were recorded with a spectral width of 6000 Hz on a JEOL JNM-GSX spectrometer operating at 500 MHz for the proton frequency. A total of 512 blocks were acquired with data points of 2K. The mixing times for the NOESY experiment were set to either 90 ms or 150 ms. ^1H–^{15}N HSQC (Bodenhausen & Ruben, 1980), double-DEPT (Wagner et al., 1989), 2D-HMQC-HOHAHA, 2D-HMQC-NOESY (Gronenborn et al., 1989), and HMQC-J (Kay & Bax, 1990) spectra were recorded with spectral widths of 5000 Hz for ^1H and 1400 Hz for ^{15}N on a Bruker AM 400 spectrometer equipped with a reverse-mode proton probe. The mixing times were set to 55 ms for the 2D-HMQC-HOHAHA experiment and to either 90 ms or 150 ms for the 2D-HMQC-NOESY experiments. 2K data points were used in the t_2 dimension, and 32–96 transients were acquired for each of 256 t_1 points. In the case of the HMQC-J experiment, 512 increments of 2K data points were collected. For the amide proton exchange experiment of FB, 1K data points were used in the t_2 dimension, and 32 transients were acquired for each of 128 t_1 points. The measurement time for one spectrum is about 80 min.

Two-dimensional spectra were obtained in the pure absorption mode with time-proportional phase incrementation (TPPI) (Marion & Wüthrich, 1983) for all heteronuclear 2D measurements and with the method of States et al. (1982) for the NOESY and PE-COSY measurements. Prior to 2D Fourier transformation, the acquired data were multiplied by a Gauss function in t_2 and by a shifted sine square function in t_1 and were zero-filled once along the t_1 direction. In the case of the PE-COSY experiment, the acquired data were also zero-filled once along the t_2 direction.

NMR samples were prepared by dissolving the purified and lyophilized FB or [^{15}N]FB in 0.4 mL of D_2O or H_2O that contains 10% D_2O at pH 5.0. The concentration of the proteins was typically 0.8–1.0 mM. The solvent resonance was suppressed by selective irradiation during the relaxation delay, which was set to 1.2 s. The probe temperature was 30 °C throughout the experiment.

Structure Calculations. All calculations were carried out on a Silicon Graphics Iris 4D/25G workstation with the programs EMBOSS (Nakai et al., manuscript in preparation) and X-PLOR (Brünger et al., 1987). The structures were calculated by the hybrid distance geometry–dynamical simulated annealing method (Nilges et al., 1988) with a few modifications (Clore et al., 1990a). Using the program EMBOSS, a set of geometrically correct substructures was generated by the metric matrix algorithm (Havel et al., 1983). After the mirror image structures were excluded from the substructures obtained from the metric matrix algorithm, dynamical simulated annealing was performed using the program X-PLOR. In order to obtain maximal experimental constraints, the iterative strategy to the structural calculation was employed (Clore et al., 1990b).

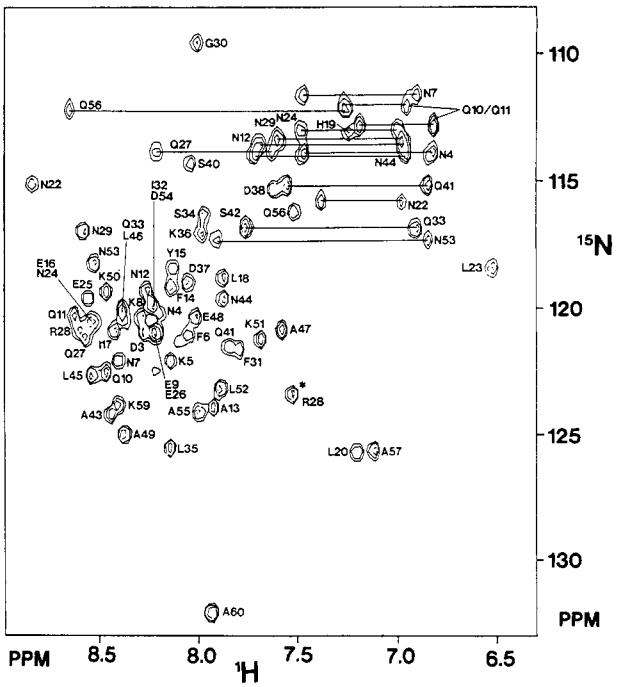

FIGURE 1: ^1H–^{15}N HSQC spectrum of [^{15}N]FB observed in H_2O at pH 5.0 and 30 °C. The protein sample was dissolved at a concentration of approximately 1.0 mM. The cross-peaks originating from the side-chain amide groups are connected by solid lines. The peak marked by the asterisk is the foldover cross-peak related to the F_1 axis originating from Arg28-NH_ϵ.

Amide Proton Exchange Experiments of the Fc-Bound FB. Lyophilized [^{15}N]FB was initially dissolved in the H_2O solution of the Fc fragment at pH 6.0 and 30 °C. A molar ratio of FB to the Fc fragment used in the present study was 1.0 to 1.0. FB is bound to the Fc fragment completely under the present condition.[2] The solution of the FB–Fc complex was diluted with D_2O, and the diluted sample solution was concentrated by ultrafiltration at pH 6.0 and 4 °C. The FB–Fc complex was incubated in D_2O for 15 min at pH 6.0 and 30 °C for the amide proton exchange. The pH of the sample solution was then adjusted to pH 3.5, and the ^1H–^{15}N HSQC spectrum of the released FB was measured in D_2O.[3] In order to obtain the reference spectrum, the sample preparation and the NMR measurement were made in the same way in the absence of the Fc fragment.

[2] In order to confirm the formation of the FB–Fc complex, we measured the ^1H–^{15}N HSQC spectrum of the FB–Fc complex in H_2O at pH 6.0 with selective irradiation of the solvent resonance. The cross-peaks observed were broad, and the intensities of the cross-peaks were reduced drastically due to spin diffusion, resulting from the formation of the FB–Fc complex (M_r 57 000).

[3] The binding of protein A to the Fc portion of IgG is affected by the pH of the solution (Ey et al., 1987). It has been demonstrated that protein A binds to the Fc portion of human IgG1 at pH 6.0 and is released at pH 3.5. It has been confirmed that FB used in the present study shows a similar pH dependence of affinity to the Fc fragment.

Table I: ^1H and ^{15}N Chemical Shifts[a] of FB at pH 5.0 and 30 °C

Main-Chain Amides					
residue	^1H	^{15}N	residue	^1H	^{15}N
Thr1			Phe31	7.78	121.6
Ala2	ND[b]	ND[b]	Ile32	8.23	119.9
Asp3	8.27	121.0	Gln33	8.38	120.3
Asn4	8.20	120.3	Ser34	7.97	116.2
Lys5	8.15	122.2	Leu35	8.14	125.6
Phe6	8.05	121.1	Lys36	7.97	117.0
Asn7	8.39	122.1	Asp37	8.05	118.9
Lys8	8.30	120.3	Asp38	7.62	115.3
Glu9	8.24	121.0	Pro39		
Gln10	8.47	122.4	Ser40	8.04	114.3
Gln11	8.62	120.3	Gln41	7.83	121.5
Asn12	8.26	119.2	Ser42	7.74	116.8
Ala13	7.92	123.9	Ala43	8.44	124.2
Phe14	8.13	119.2	Asn44	7.88	119.7
Tyr15	8.10	118.4	Leu45	8.54	122.7
Glu16	8.55	120.5	Leu46	8.37	120.0
Ile17	8.42	120.8	Ala47	7.56	120.8
Leu18	7.86	118.7	Glu48	8.02	120.3
His19	7.23	113.0	Ala49	8.37	125.0
Leu20	7.18	125.7	Lys50	8.46	119.4
Pro21			Lys51	7.67	121.2
Asn22	8.84	115.1	Leu52	7.88	123.2
Leu23	6.49	118.4	Asn53	8.53	118.1
Asn24	8.52	120.5	Asp54	8.24	119.9
Glu25	8.56	119.6	Ala55	7.98	124.0
Glu26	8.20	121.5	Gln56	7.50	116.2
Gln27	8.58	121.1	Ala57	7.10	125.7
Arg28	8.61	120.8	Pro58		
Asn29	8.59	116.9	Lys59	8.41	123.8
Gly30	8.00	109.5	Ala60	7.94	132.1

Side-Chain Amides							
	^1H				^1H		
residue	δ^1	δ^2	^{15}N	residue	ϵ^1	ϵ^2	^{15}N
Asn7	6.89	7.47	111.6	Gln33	6.89	7.77	116.8
Asn24	6.99	7.48	113.0	Gln41	6.83	7.55	115.1
Asn53	6.83	7.90	117.3				

residue	^1H, δ	^{15}N	residue	^1H, ϵ	^{15}N
Asn4	6.80, 7.46	113.8	Gln10/11[c]	6.80, 7.18	112.7
Asn12	6.96, 7.69	113.5	Gln10/11[c]	6.95, 7.27	112.1
Asn22	6.96, 7.38	115.7	Gln27	7.63, 8.21	113.8
Asn29	6.96, 7.59	113.3	Gln56	7.28, 8.68	112.2
Asn44	6.95, 7.72	114.0			

[a] Chemical shifts of ^1H and ^{15}N are expressed in ppm relative to DSS and liquid ammonia, respectively. [b] Not detectable. [c] In the case of Gln10 and Gln11, the chemical shifts of the C_γ protons were overlapped. The resonances originating from the side-chain amide groups of Gln10 and Gln11 could not be assigned in a site-specific way.

RESULTS

Assignments of the Amide Groups of FB. Figure 1 shows the amide region of the ^1H–^{15}N HSQC spectrum of [^{15}N]FB observed in H_2O at pH 5.0 and 30 °C. All of the cross-peaks originating from the amide groups of the backbone and the side chains of FB except for Ala2 were observed in the ^1H–^{15}N HSQC spectrum. In order to detect the resonances of the amide groups of the side chains of the Asn and Gln residues, the double-DEPT spectrum was also measured (data not shown).

In a previous paper, all the amide proton resonances of the backbone of FB except for the resonance of Ala2 have been assigned (Torigoe et al., 1990). Therefore, on the basis of the established assignment of the amide proton resonances, it was possible to assign the cross-peaks of the ^1H–^{15}N HSQC spectrum of [^{15}N]FB. In the case of the cross-peaks which were not possible to assign due to the degeneracy of the amide proton resonances, we used the connectivities between the amide proton and the C_α proton and between the amide proton and the C_β proton obtained by the ^1H–^{15}N HMQC-HOHAHA spectrum. The assignments of the cross-peaks were also confirmed in a sequential manner by observing the ^1H–^{15}N HMQC-NOESY spectrum (data not shown).

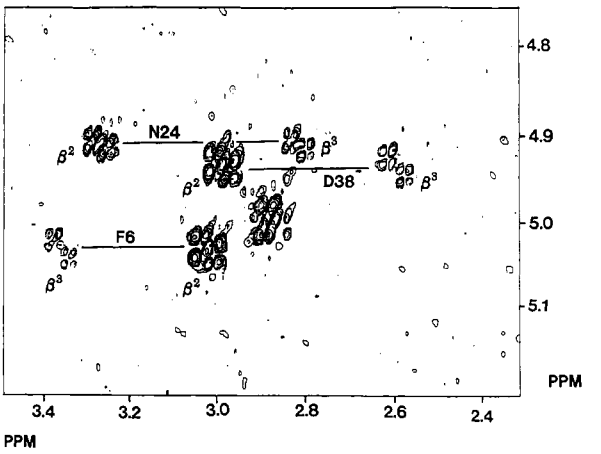

FIGURE 2: Portion of the PE-COSY spectrum of FB observed in D_2O at pH 5.0 and 30 °C.

FB contains eight Asn and six Gln residues. In the present study, the assignments of the individual amide proton resonances originating from the side chains of the Asn and Gln residues have been established by observing NOEs between NH_δ and $C_\beta H$ for the Asn residues and NOEs between NH_ϵ and $C_\gamma H$ for the Gln residues; a mixing time of 90 ms was used for these experiments (Montelione et al., 1992). The side-chain amide proton resonances of Asn7, Asn24, Gln33, Gln41, and Asn53 have been assigned individually. Table I summarizes the ^1H and ^{15}N chemical shifts of the amide groups of FB observed at pH 5.0 and 30 °C.

Stereospecific Assignments of the C_β Protons. We have established the stereospecific assignments by using $^3J_{\alpha\beta}$ coupling constants combined with the intraresidual NH–$C_\beta H$ NOEs observed with a mixing time of 90 ms (Hyberts et al., 1987). $^3J_{\alpha\beta}$ coupling constants were determined by observing the PE-COSY spectrum in D_2O, in which the cross-peaks gave the passive coupling between C_α and C_β protons (Figure 2).

Of 60 amino acids residues in FB, 26 have nondegenerate C_β proton resonances, excluding the Pro residues. For 13 of the 26 nondegenerate C_β protons, it was possible to obtain $^3J_{\alpha\beta}$ coupling constants and NH–$C_\beta H$ NOEs from PE-COSY and NOESY experiments, respectively. All $^3J_{\alpha\beta}$ coupling constants obtained in the present study were <5 Hz or >10 Hz, indicating that the conformation of the C_α–C_β bond of the side chains takes a unique staggered rotamer. On the basis of the $^3J_{\alpha\beta}$ coupling constants and the intensities of NH–$C_\beta H$ NOEs, we have establsihed stereospecific assignments of C_β protons for 13 residues, i.e., Phe6, Asn7, Leu18, His19, Leu20, Leu23, Asn24, Asn29, Asp38, Gln41, Leu45, Asn53, and Gln56.

Experimental Constraints for Structure Calculations. Interproton distance constraints were obtained from the NOESY and ^1H–^{15}N HMQC-NOESY spectra observed with mixing times of either 90 ms or 150 ms in both cases. Quantitative determination of the cross-peak intensities was based on the counting of the exponentially spaced counterlevels. Observed NOE data were classified into four distance ranges, 1.8–2.5, 1.8–3.0, 1.8–4.0, and 1.8–5.0 Å, corresponding to very strong, strong, medium, and weak NOEs, respectively (Montelione et al., 1992). Pseudoatoms were used for the

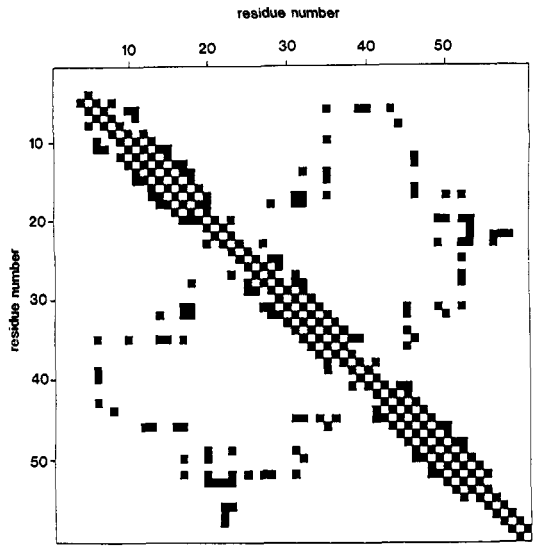

FIGURE 3: Diagonal plot of NOEs observed in FB in solution. The two axes are labeled with the residue number of FB. The square indicates that NOE was observed between residues at positions shown along the axis.

Table II

(A) Structural Statistics and Atomic RMS Differences

	10 converged structures	⟨mean⟩ structure[a]
RMS deviations from exptl distance constraints (Å)	0.055 ± 0.003	0.052
RMS deviations from exptl dihedral constraints (deg)	1.2 ± 0.5	2.4
F_{NOE} (kcal mol^{-1})[b]	94.4 ± 9.8	84.6
F_{tor} (kcal mol^{-1})[b]	5.53 ± 3.97	8.28
F_{repel} (kcal mol^{-1})[b]	74.0 ± 5.9	70.4
E_{L-J} (kcal mol^{-1})[c]	−231.5 ± 9.0	−238.1
RMS deviations from idealized covalent geometry		
bonds (Å)	0.009 ± 0.0004	0.009
angles (deg)	1.960 ± 0.011	1.966
impropers (deg)	1.230 ± 0.033	1.237

(B) Atomic RMS Differences of 10 Converged Structures versus Mean Structure[d] (Å)

	residues 10–55
backbone (N, C_α, C, O)	0.52 ± 0.10
all heavy atoms	0.98 ± 0.08

[a] ⟨mean⟩ structure is the restrained minimized structure obtained by the averaged coordinates of the 10 converged structures. [b] F_{NOE}, F_{tor}, and F_{repel} are the energies related to the NOE violations, the torsion angle violations, and the van der Waals repulsion term, respectively. The force constants of these terms used were the standard values (Clore et al., 1986). [c] E_{L-J} is the Lennard–Jones van der Waals energy calculated with the CHARMm empirical energy function (Brooks et al., 1983). E_{L-J} was not used in the dynamical simulated annealing calculations. [d] Mean structure was obtained by the averaged coordinates of the 10 converged structures.

prochiral methylene protons that had not been assigned in a stereospecific way, the methyl groups of the Leu residues, and the C_α protons of Gly30 (Wüthrich et al., 1983). Correction factors for the use of pseudoatoms were added to the distance constraints.

A set of 587 interproton distance constraints were obtained. The distance constraints consisted of 205 intraresidue NOEs and 173 sequential ($|i-j| = 1$), 101 short-range ($1 < |i-j| \leq 5$), and 108 long-range ($|i-j| > 5$) interresidue NOEs. The NOE connectivities are shown in Figure 3.

The $^3J_{HN\alpha}$ coupling constants were measured using the HMQC-J spectrum of [^{15}N]FB (data not shown) and corrected

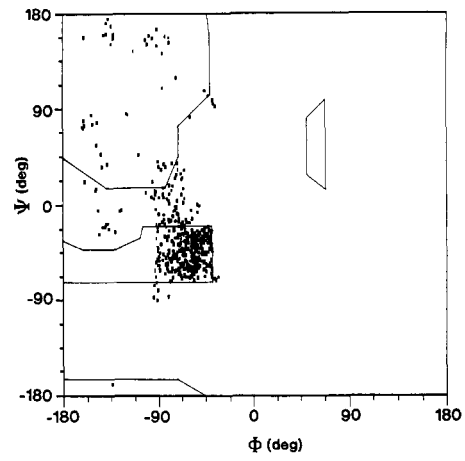

FIGURE 4: Ramachandran-type plot for the residues from Gln10 to Ala55 of the 10 converged structures of FB.

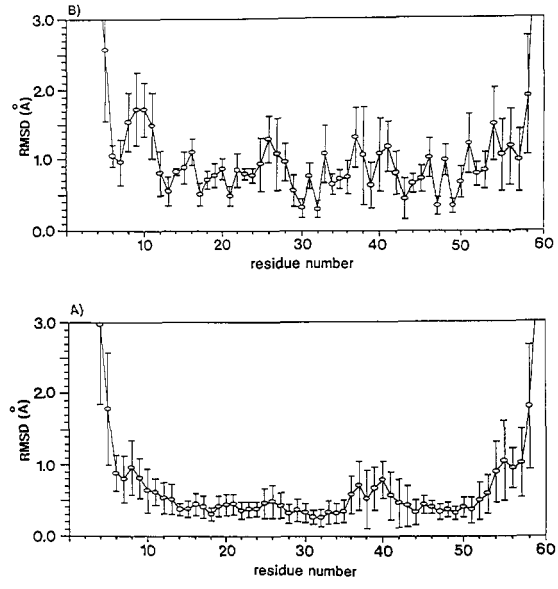

FIGURE 5: Distribution of atomic RMSD of the backbone (A) and the all-heavy atoms (B) for the 10 converged structures about the mean structure as a function of the residue number. The bars indicate the standard deviations in these values.

according to the method of Kay and Bax (1990). A corrected $^3J_{HN\alpha}$ greater than 8 Hz constrained the ϕ angle in the range of $-120 \pm 40°$, and a corrected $^3J_{HN\alpha}$ less than 5 Hz constrained in the range of $-65 \pm 25°$ (Wagner et al., 1987). For t^2g^3, g^2g^3, and g^2t^3 staggered conformations of the side chain, the χ^1 angle was constrained in the range of $-60 \pm 40°$, $60 \pm 40°$, and $180 \pm 40°$, respectively.

We initially calculated the polypeptide fold by using the distance and torsion angle constrains obtained as described above. The positions of the hydrogen bonds have been determined on the basis of the preliminary polypeptide fold, along with the results of the amide proton exchange experiments. As a result of this analysis, a total of 23 hydrogen bonds related to α-helices and 1 hydrogen bond related to a β-turn have been identified. Hydrogen bond constraints for the α-helices and the β-turn were added as distance constraints, NH_i–O_j and N_i–O_j, whose target values were set to 1.7–2.3 and 2.4–3.3 Å, respectively.

The final structures were calculated on the basis of 692 experimental constraints, which comprised 587 interproton distance constraints, 57 torsion angle constraints (involving 44 ϕ and 13 χ^1 torsion angles), and 48 distance constraints related to hydrogen bonds in the α-helices and the β-turn.

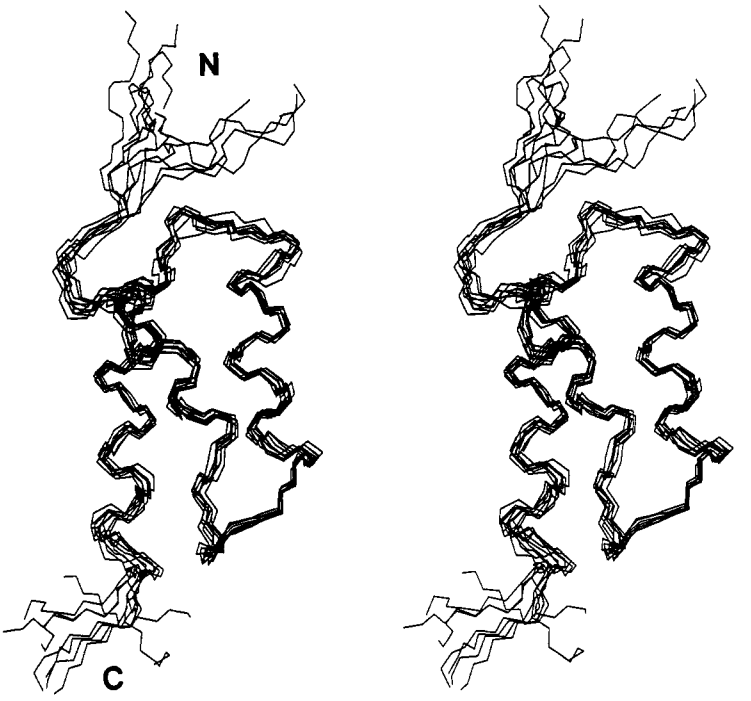

FIGURE 6: Stereopair of the superpositions of the 10 converged structures of FB. These are the results of the best fit of the N, C_α, C, and O atoms for the Gln10–Ala55 segment. Only the backbone (N, C_α, and C) is shown.

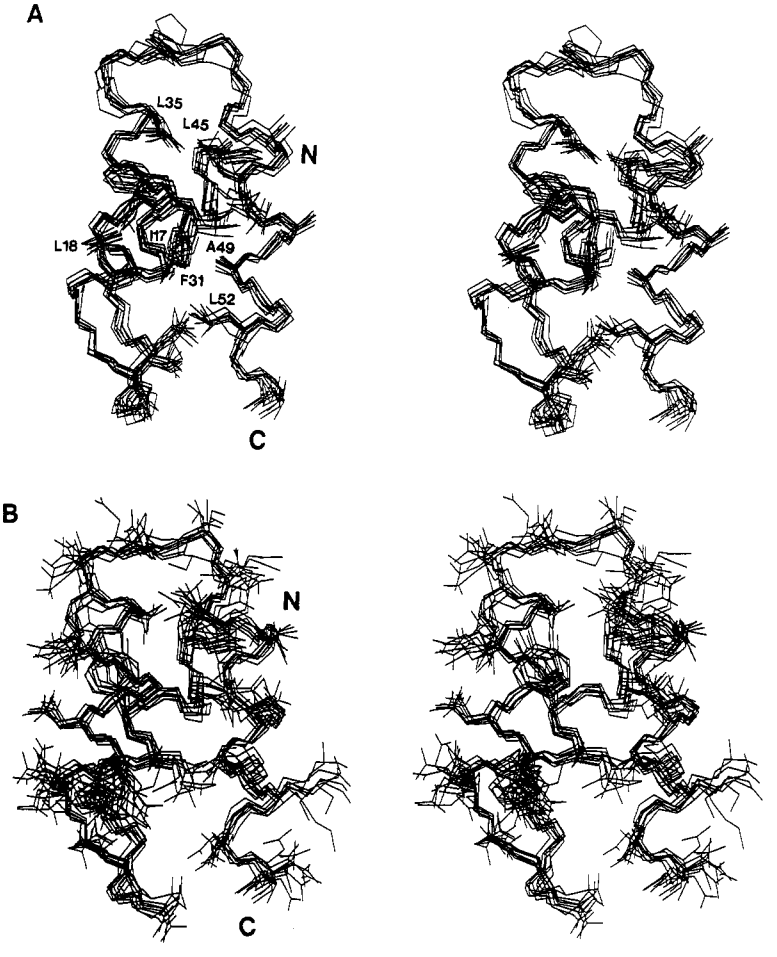

FIGURE 7: Stereopairs of the superposition of the 10 converged structures of FB for the Gln10–Ala55 segment. Side-chain atoms are shown for the hydrophobic amino acids residues (A) and the hydrophilic amino acid residues (B).

Structure Calculations and Evaluation. At first, we carried out the distance geometry calculation by starting from 55 initial structures of FB. This calculation resulted in 41 solutions, which had correct polypeptide folds excluding 14 mirror-image substructures. Next, the dynamical simulated annealing calculations were performed by using these 41 substructures. The distance and torsion angle violations of the 41 solutions obtained by dynamical simulated annealing

calculations are smaller than 0.6 Å and 27°, respectively. Of the 41 solutions, we selected 10 solutions that had the distance and torsion angle violations of smaller than 0.5 Å and 10°, respectively.

Structural statistics for the 10 converged structures and atomic RMSDs are given in Table II. The final 10 converged structures exhibit an atomic RMSD about the averaged coordinate positions of 0.52 ± 0.10 Å for the backbone atoms and 0.98 ± 0.08 Å for all heavy atoms, excluding the N-terminal (Thr1–Glu9) and C-terminal (Gln56–Ala60) residues. The deviations from idealized covalent geometry were very small, and the Lennard–Jones van der Waals energy is large and negative, indicating that no distortions and bad contacts exist in the converged structures. In a Ramachandran-type plot (Figure 4), the dihedral backbone angles for the residues from Gln10 to Ala55 of the final 10 converged structures fall either in the helix region or in the generally allowed regions.

Figure 5 shows the distribution of the atomic RMSD for the 10 individual converged structures about the mean structure as a function of the residue number. Except for the N- and C-terminal segments, which are disordered, the structure of the backbone from Gln10 to Ala55 is defined very well (Figure 5A). However, the atomic RMSD of the all-heavy atoms for each of Gln10, Gln11, Glu26, Asp37, Lys51, and Asp54 is greater than 1.2 Å (Figure 5B). These residues exist at the surface of the molecule. This indicates that the side chains of these surface residues are disordered in solution.

Description of the Polypeptide Fold of FB in Solution. Figure 6 shows the stereopair of the best-fit superposition of the backbone atoms for the 10 converged structures.[4] FB consists of three α-helices, i.e., helix I (Gln10–His19), helix II (Glu25–Asp37), and helix III (Ser42–Ala55). These three helices are connected by turn structures. The type I β-turn, which is characterized by the hydrogen bond between Leu23 NH and Leu20 CO, is formed between helix I and helix II.

All of the hydrophobic amino acids of FB except for Ala2, Ala47, Ala55, and Ala60 are buried in the interior of the bundle of the three helices and form a hydrophobic core (Figure 7A), whereas most of the hydrophilic residues are located at the surface of the molecule (Figure 7B).

Amide Proton Exchange Experiments for the Fc-Bound FB. Figure 8A shows the ^1H–^{15}N HSQC spectrum of the free [^{15}N]FB observed in H_2O at pH 3.5 and 30 °C. The spectral assignments established by ^1H–^{15}N HMQC-HOHAHA and ^1H–^{15}N HMQC-NOESY experiments are given in the figure. In order to obtain information about the secondary structure of the Fc-bound FB in solution, the amide proton exchange experiments were made by incubating the Fc-bound FB in D_2O for 15 min at pH 6.0 and 30 °C. After incubation, the pH of the protein solution was lowered to 3.5 to dissociate the complex, and the ^1H–^{15}N HSQC spectrum of the dissociated FB was measured. As a reference, a similar experiment was performed for [^{15}N]FB in the absence of the Fc fragment. Figure 8B,C shows the results for the amide proton exchange experiments for FB performed in the presence and absence of the Fc fragment, respectively.

DISCUSSION

Three-Dimensional Solution Structure of FB in the Free State. In the present study, we have determined the three-

[4] The coordinates of the 10 converged structures, together with the complete list of experimental NMR constraints, will be deposited in the Brookhaven Protein Data Bank.

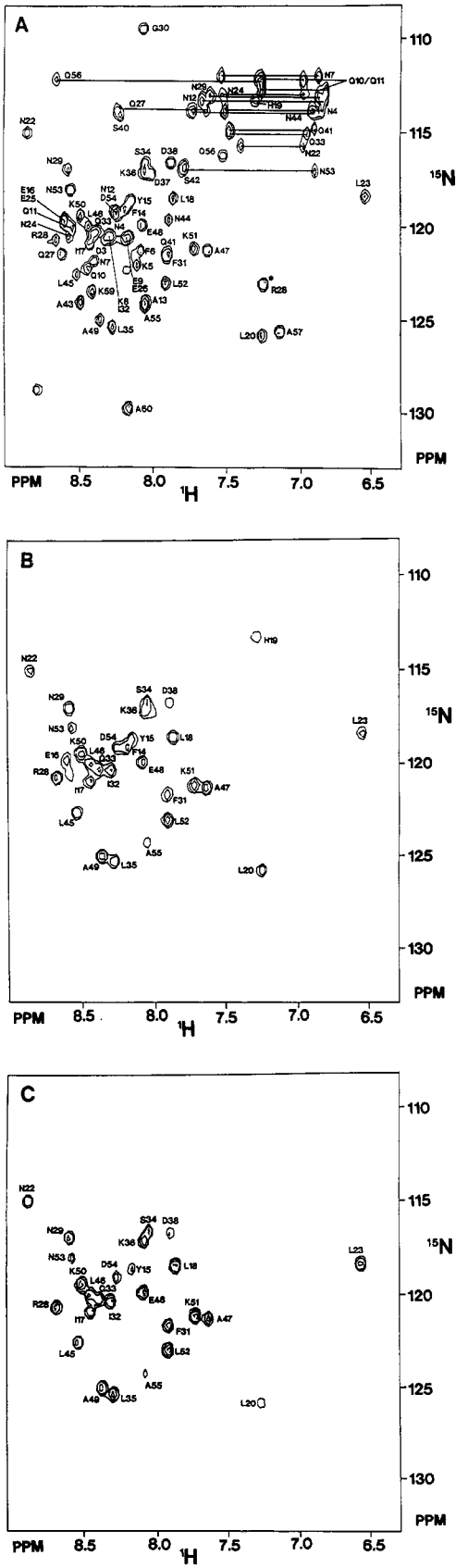

FIGURE 8: (A) ^1H–^{15}N HSQC spectrum of [^{15}N]FB observed in H_2O at pH 3.5 and 30 °C. The peak marked by the asterisk is the foldover cross-peak related to the F_1 axis originating from Arg28-NH_ϵ. (B) ^1H–^{15}N HSQC spectrum of [^{15}N]FB preincubated in D_2O at pH 6.0 and 30 °C for 15 min in the presence of the Fc fragment; the spectrum was measured in D_2O at pH 3.5 and 30 °C. (C) ^1H–^{15}N HSQC spectrum of [^{15}N]FB preincubated as in (B) but in the absence of the Fc fragment; the spectrum was measured in D_2O at pH 3.5 and 30 °C.

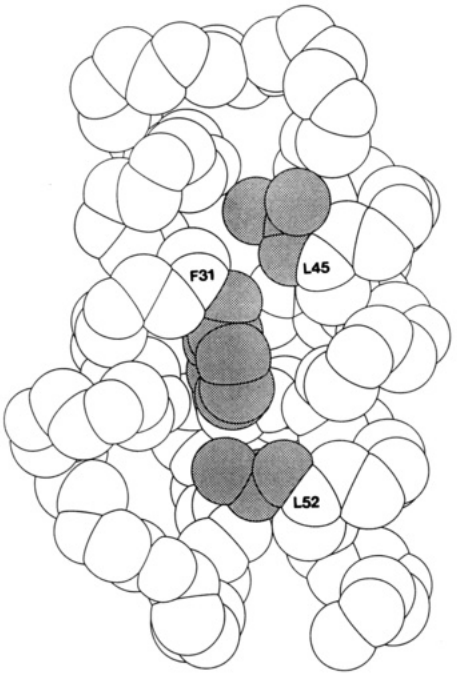

FIGURE 9: Space-filling representation of the mean structure for the Gln10–Ala55 segment of the free FB in solution.

dimensional solution structure of the free FB by NMR and hybrid distance geometry–dynamical simulated annealing calculations. It has been shown that the free FB consists of three α-helices, helix I, helix II, and helix III. Of the three helices, helix II and helix III contact most intimately with each other; Phe31 and Leu35 (helix II) and Leu45, Ala49, and Leu52 (helix III) are involved in the contact of the two helices (Figure 7A). It should particularly be noted that the side chain of Phe31 is *sandwiched* by those of Leu45 and Leu52 (Figure 9). The interactions observed between helix II and helix III of FB are reminiscent of those characterized by the *coiled-coil* interaction which has been exhibited by tropomyosin (McLachlan et al., 1975).

A variety of truncated analogues of FB have been expressed by recombinant DNA technology (Huston et al., 1992). It has been indicated that a truncated analogue of FB, in which the segment from Asp38 to Lys59 corresponding to the helix III region is deleted, binds to the monomeric IgG with greatly reduced affinity. This result strongly suggests that helix III is essential to the formation of the global chain fold of FB in solution. It is possible that the structure of the truncated analogue of FB is significantly different from that of the intact FB and therefore the mode of interactions with Fc is different for these proteins.

Comparisons of the X-ray and NMR Structures of the Fc-Bound FB. The crystal data indicated that two helical regions, Gln10–Leu18 and Glu26–Asp37, exist in the Fc-bound FB and the Ser42–Glu48 segment is extended with no structural information available in the Ala49–Lys59 segment (Deisenhofer, 1981). Figure 10 compares the schematic ribbon drawing of the structure of the free FB in solution with that of the Fc-bound FB in the crystal. In the free FB in solution, helix II and helix III are oriented antiparallel to each other, whereas the long axis of helix I is tilted at an angle of 30° with respect to those of helix II and helix III. By contrast, the first helical region (Gln10–Leu18) and the second helical region (Glu26–Asp37) are antiparallel to each other in the crystal.

The backbone RMSD for the Gln10–Asp37 segment between the solution structure of the free FB and the crystal

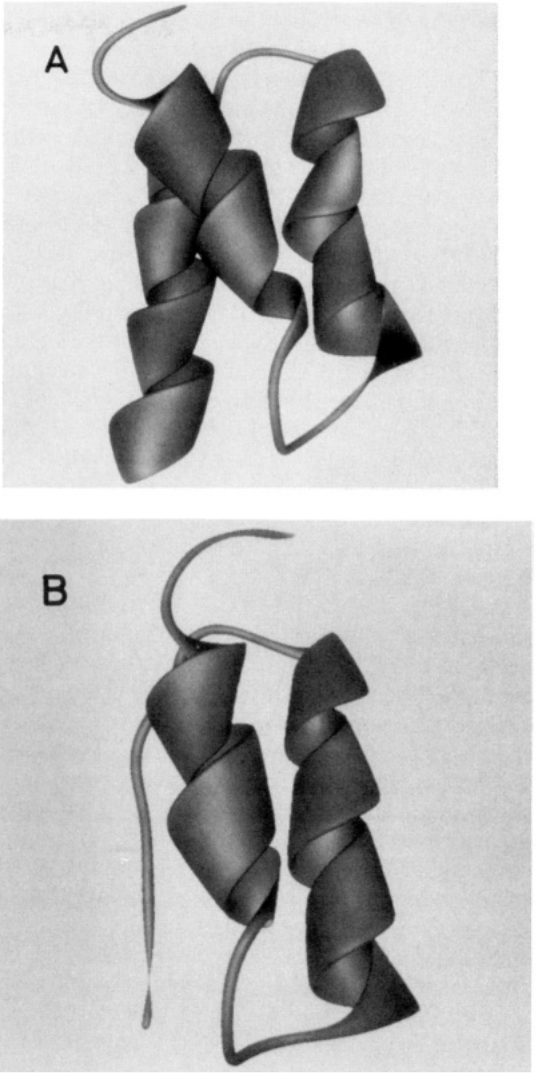

FIGURE 10: Schematic ribbon drawing of (A) the mean structure of the Phe6–Ala55 segment of the free FB in solution and (B) the Phe6–Glu48 segment of the crystal structure of the Fc-bound FB.

structure of the Fc-bound FB was 1.56 Å. As far as the backbone atoms for the Gln10–Asp37 segment are concerned, the solution structure of FB in the free state and the crystal structure of the Fc-bound FB are almost identical. However, the difference of the orientation of the side chains of Tyr15, Ile17, and Leu18, all of which exist in helix I, is observed between the solution and the crystal structures. The side chains of Ile17 and Leu18 are buried in the hydrophobic core of the free FB in solution (see Figure 7A). In the crystal, the side chains of Tyr15, Ile17, and Leu18 exist at the interface of FB and the Fc fragment and are in close spatial proximity to hydrophobic residues of the Fc fragment, indicating that the hydrophobic interaction exists in the Fc–FB complex.

Figure 8B,C shows ^{1}H–^{15}N HSQC spectra for FB observed in the presence and absence of Fc, respectively. This result indicates that the cross-peaks originating from Phe14, Glu16, and His19 (helix I) can only be detected in the case of the Fc-bound FB. These results suggest that the amide proton exchange rates for Phe14, Glu16, and His19 became slower upon formation of the FB–Fc complex. We therefore conclude that Phe14, Glu16, and His19 are located at the binding site of FB to the Fc fragment. The results obtained from NMR data are quite consistent with the crystal data which indicate that the helical region from Gln10 to Leu18 is primarily responsible for the formation of the Fc–FB complex.

It has been reported that the exchange rate for the amide group in the random coil is 10 min^{-1} at pH 6.0 and 25 °C (Wüthrich, 1986). This means that the incubation time of 15 min at 30 °C used in the present study for the Fc-bound FB is long enough to complete the amide proton exchange for the disordered segment. In the present study, it has been shown that the cross-peaks originating from the residues of the C- and N-terminal segments, which are disordered in solution, disappeared within 15 min (Figure 8B,C).

In the amide proton exchange experiments, the cross-peaks originating from the Leu45–Ala55 segment (helix III) were observed in the ^{1}H–^{15}N HSQC spectra of both the free FB and the Fc-bound FB (Figure 8B,C). This result clearly indicates that the amide proton exchange rates for the helix III residues are not affected by the binding of the Fc fragment. Therefore, we conclude that helix III is retained in the Fc-bound FB in solution. This result is in marked contrast to the crystal data of the Fc-bound FB, where a third helix, which corresponds to helix III in the free FB, does not exist (Deisenhofer, 1981).

It has been demonstrated that FB forms two contacts (contact 1 and contact 2) with the Fc fragment in the crystal (Deisenhofer, 1981). Contact 1 consists of the residues existing in the first helical region (Gln10–Leu18) and the second helical region (Glu26–Asp37) and those existing in the C_H2 and C_H3 domains of the Fc fragment. It has been shown that Gln33, Ser34, and Asp37, which are located in the C-terminal segment of the second helical region, and Asp38 and Gln41 that follow are covered by the formation of contact 2. It has been suggested that FB is bound to the Fc fragment at contact 1 in solution and contact 2 is a crystal contact (Deisenhofer, 1981). We therefore suggest that contact 2 is responsible for the unfolding of the Ser42–Ala55 segment in the crystal.

In order to investigate the interaction of FB with the Fc fragment in more detail, ^{13}C and ^{15}N NMR studies using the ^{13}C-labeled Fc analogues and [^{15}N]FB are under way in our laboratory.

ACKNOWLEDGMENT

We thank Dr. K. Nagayama for the useful discussions at the initial stage of the structural calculation, Dr. H. Nakamura for providing us with the program EMBOSS, and S. Masuda for his help in the analyses of some of the NMR data.

REFERENCES

Bodenhausen, G., & Ruben, D. J. (1980) *Chem. Phys. Lett. 69*, 185–189.

Brooks, B. R., Bruccoleri, R. E., Olafson, B. D., States, D. J., Swaminathan, S., & Karplus, M. (1983) *J. Comput. Chem. 7*, 165–175.

Brünger, A. T., Clore, G. M., & Karplus, M. (1987) *Protein Eng. 1*, 399–406.

Clore, G. M., Nilges, M., Sukumaran, D. K., Brünger, A. T., Karplus, M., & Gronenborn, A. M. (1986) *EMBO J. 5*, 2729–2735.

Clore, G. M., Driscoll, P. C., Wingfield, P. T., & Gronenborn, A. M. (1990a) *J. Mol. Biol. 214*, 811–817.

Clore, G. M., Appella, E., Yamada, M., Matsushima, K., & Gronenborn, A. M. (1990b) *Biochemistry 29*, 1689–1696.

Deisenhofer, J. (1981) *Biochemistry 20*, 2361–2370.

Ey, P. L., Prowse, S. J., & Jenkin, C. R. (1978) *Immunochemistry 15*, 429–436.

Gronenborn, A. M., Bax, A., Wingfield, P. T., & Clore, G. M. (1989) *FEBS Lett. 243*, 93–98.

Havel, T. F., Kuntz, I. D., & Crippen, G. M. (1983) *Bull. Math. Biol. 45*, 665–720.

Huston, J. S., Cohen, C., Maratea, D., Fields, F., Tai, M.-S., Cabaral-Denison, N., Juffras, R., Rueger, D. C., Ridge, R. J., Oppermann, H., Keck, P., & Baird, L. G. (1992) *Biophys. J. 82*, 105–109.

Hyberts, S. G., Märki, W., & Wagner, G. (1987) *Eur. J. Biochem. 164*, 625–635.

Jeener, J., Meier, B. H., Bachmann, P., & Ernst, R. R. (1979) *J. Chem. Phys. 71*, 4546–4553.

Kay, L. E., & Bax, A. (1990) *J. Magn. Reson. 86*, 110–126.

Langone, J. J. (1982) *Adv. Immunol. 32*, 157–252.

Marion, D., & Wüthrich, K. (1983) *Biochem. Biophys. Res. Commun. 113*, 967–974.

McLachlan, A. D., & Stewart, M. (1975) *J. Mol. Biol. 98*, 293–304.

Moks, T., Abrahmsen, L., Nilsson, B., Hellman, U., Sjoquist, J., & Uhlen, M. (1986) *Eur. J. Biochem. 156*, 637–643.

Montelione, G. T., Wüthrich, K., Burgess, A. W., Nice, E. C., Wagner, G., Gibson, K. D., & Scherager, A. (1992) *Biochemistry 31*, 236–249.

Mueller, L. (1987) *J. Magn. Reson. 72*, 191–196.

Nilges, M., Clore, G. M., & Gronenborn, A. M. (1988) *FEBS Lett. 229*, 317–324.

Saito, A., Honda, S., Nishi, T., Koike, M., Ozaki, K., Itoh, S., & Sato, M. (1989) *Protein Eng. 2*, 481–487.

Sjodahl, J. (1977a) *Eur. J. Biochem. 73*, 343–351.

Sjodahl, J. (1977b) *Eur. J. Biochem. 78*, 471–490.

States, D. J., Haberkorn, R. A., & Ruben, D. J. (1982) *J. Magn. Reson. 48*, 286–292.

Torigoe, H., Shimada, I., Saito, A., Sato, M., & Arata, Y. (1990) *Biochemistry 29*, 8787–8793.

Wagner, G. (1989) *Methods Enzymol. 176*, 93–113.

Wagner, G., Braun, W., Havel, T., Schaumann, T., Go, N., & Wüthrich, K. (1987) *J. Mol. Biol. 196*, 611–639.

Wüthrich, K. (1986) *NMR of Proteins and Nucleic Acids*, John Wiley, New York.

Wüthrich, K., Billeter, M., & Brawn, W. (1983) *J. Mol. Biol. 169*, 949–961.